

Component sizing optimization of plug-in hybrid electric vehicles

Xiaolan Wu^{*}, Binggang Cao, Xueyan Li, Jun Xu, Xiaolong Ren

School of Mechanical Engineering, Xi'an Jiaotong University, Xi'an, 710049, China

ARTICLE INFO

Article history:

Received 26 November 2009
Received in revised form 6 July 2010
Accepted 22 August 2010

Keywords:

Optimization
Plug-in hybrid electric vehicle
Chaos optimization algorithm
Component sizes
All electric range
Cost

ABSTRACT

Plug-in hybrid electric vehicles (PHEVs) are considered as one of the most promising means to improve the near-term sustainability of the transportation and stationary energy sectors. This paper describes a methodology for the optimization of PHEVs component sizing using parallel chaos optimization algorithm (PCOA). In this approach, the objective function is defined so as to minimize the drivetrain cost. In addition, the driving performance requirements are considered as constraints. Finally, the optimization process is performed over three different all electric range (AER) and two types of batteries. The results from computer simulation show the effectiveness of the approach and the reduction in drivetrain cost while ensuring the vehicle performance.

© 2010 Elsevier Ltd. All rights reserved.

1. Introduction

In recent years new, eco-friendly, technology within the automotive industry has been focusing on the realization of zero pollution and the development of green vehicles by increasing system energy efficiency and significantly reducing exhaust emissions [1]. Electric vehicles (EVs), which are more energy efficient, have zero tail pipe emissions. However, these vehicles have not been successful because of higher cost, added weight of batteries, reduced load capacity, limited range and lack of recharging infrastructure. Conventional hybrid electric vehicles (HEVs) offer improved fuel economy, low emissions and take the advantage of existing fuel infrastructure, but, still depend entirely on petroleum to charge the battery pack [2]. Plug-in hybrid electric vehicles (PHEVs) use both electrochemical energy storage and a conventional fuel to overcome the weaknesses of EVs and HEVs.

Plug-in hybrid electric vehicles (PHEVs) are hybrid electric vehicles that can draw and store energy from an electric grid to supply propulsive energy for the vehicle. This simple functional change to the conventional HEV allows a PHEV to displace petroleum energy with multi-source electrical energy. And it has important and generally beneficial impacts on transportation energy sector petroleum consumption, criteria emissions output, and carbon dioxide emissions, as well as on the performance and makeup of the electrical grid. Because of these characteristics and their near-term

availability, PHEVs are considered as one of the most promising means to improve the near-term sustainability of the transportation and stationary energy sectors [3].

Proper execution of a successful PHEV design requires its key mechanical and electrical components sizing. The studies of PHEV component sizing found in the open literature are mainly performed manually and analytically by the designer. Simpson [4] analyzed the component sizes using the PAMVEC model. Sharer et al. [5] developed an automated sizing process. According to the vehicle performance requirements, the engine, motor and battery size are obtained by simulation tool PSAT. Golbuff [6] proposed an analysis-based design optimization for component sizing in PHEV. However, a systemic design using optimization algorithm has not been published.

Whereas, PHEV is a complex electro-mechanical system and the interaction between the various components makes it difficult to size specific components manually or analytically. So, proper execution of a successful PHEV design requires optimal sizing of the key mechanical and electrical components by using optimization algorithm and simulation techniques. The optimization algorithm tries to minimize the objective function (drivetrain cost in our case) by searching the multidimensional parameter space for various combinations of the design variables and selecting the best combination at each iteration. In addition, using simulation tool, the optimization algorithm works together (looped) with a computer simulation model to obtain an optimal solution. Due to the highly non-linear and non-smooth characteristics of the drivetrain system, this optimization problem may have a large number of local optimums and some constraints may contain quite pronounced

^{*} Corresponding author.

E-mail address: wuxiaolan.2008@yahoo.com.cn (X. Wu).

noise [7]. So, the gradient-based optimization methods may not converge to a global solution and therefore a non-gradient-based optimization algorithm is proposed.

Chaos, apparently disordered behavior that is nonetheless deterministic, is a universal phenomenon that occurs in many systems in all areas of science [8]. The chaos optimization algorithm (COA) is based on ergodicity, stochastic properties and regularity of the chaos [9]. Unlike some stochastic optimization algorithms, such as GA, which escape from local minima by accepting some bad solutions according to certain probability, the COA searches on the regularity of chaotic motion [10]. Furthermore, the COA is more capable of hill-climbing and escaping from local optima than the existing stochastic searching algorithm. However, the COA has the characteristic of the sensitive dependence to initial conditions, tiny difference in initial value, and there may be carrying completely different searching process. So, in some conditions, it may take much search time to find the optimum solution, especially for complex optimization problem. To overcome this drawback, parallel chaos optimization algorithm (PCOA) is proposed, which is an improved chaos optimization algorithm and can solve complex optimization problem by searching synchronously from several initial points [11]. Moreover, all merits of COA are completely inherited including the features of easy implementation, short execution time and robust mechanisms of escaping from local optimum. Therefore, PCOA is one of the effective and rapid optimization algorithms for complex optimization problem.

In this paper, PCOA is proposed to find the optimal component sizes in PHEV. Considering the effects of cost and performance on the marketability of PHEVs, the objective function is defined to minimize drivetrain cost and driving performance requirements are selected as constraints to ensure that the vehicle performance is not sacrificed during the optimization. In addition, the advanced vehicle simulator (ADVISOR) [12] is used as the simulation tool to study the optimization process, which evaluates the performance of a vehicle in a combined backward–forward facing approach [13]. The simulation results are finally obtained to investigate the effectiveness of the approach and the effects of battery type, driving cycle and performance requirement on the component sizing optimization of PHEVs.

2. Vehicle configuration

PHEVs have a drivetrain that incorporates electric motor and internal combustion (IC) engine, and like conventional HEVs these components can be arranged in series, parallel, or split series/parallel configurations [14]. In the parallel configuration (shown in Fig. 1), both electric motor and IC engine may deliver power to the vehicle wheels. The electric motor may also be used as a generator to charge the battery by either the regenerative braking or absorbing the excess power from the engine when its output is greater than that is required to drive the wheels. The main advantage of parallel PHEV is its improved dynamic performance due to

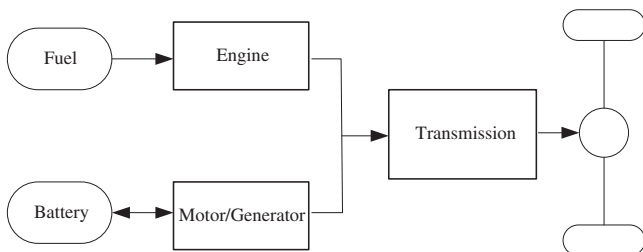


Fig. 1. Parallel HEV configuration.

direct coupling between the IC engine and electric motor. This feature makes the parallel PHEV more suitable for passenger cars. This paper selects the parallel configuration for studying.

3. PHEV component sizing optimization

3.1. Optimization variables

The drivetrain of a parallel PHEV is a link of IC engine, electric motor, transmission, wheels and axles and battery pack. Among them, the IC engine, electric motor and energy storage system are considered as the most critical components. Proper selection of these components would significantly affect characteristics and performance of the vehicle.

To consider the effect of component sizes on the optimization of PHEV design, a baseline is selected for the engine and electric motor. The sizes of corresponding component are varied during the design process using the varied scaling factors and baseline. Torque scaling factors of IC engine and motor ($S_{IC,SEM}$) are respectively used for modifying the IC engine and motor sizes. For the energy storage system, a battery pack is selected as the baseline, battery modules number (N_{BM}) and capacity scaling factor (S_{BC}) are varied during the optimization.

3.2. Optimization problem formulation

As mentioned previously, the PHEV design in this work is aimed to minimize the drivetrain cost and maintain driving performance. Furthermore, in order to simplify this optimization problem, the drivetrain cost only includes the component cost of engine, motor and battery. Assuming other components are the same for all types of PHEV and ignoring their costs, such as charger, vehicle frames and transmission, the objective function is defined as follows:

$$f(x) = \$C_E + \$C_M + \$C_{Batt} + \$C_{BattRep} \quad (1)$$

where $\$C_E$ is the engine cost, $\$C_M$ is the cost of electric motor and power electronics, $\$C_{Batt}$ is the battery pack cost including batteries and accessories, $\$C_{BattRep}$ is the battery replacement cost. The component costs estimation method is from EPRI and Sam Golbuff study [6,15,16], which can be expressed as follows:

$$\$C_E = \$12.00 * P_E + \$424 \quad (2)$$

$$\$C_M = \$21.775 * P_M + \$425 \quad (3)$$

$$\$C_{Batt,NiMH} = \$321.2 * \text{energy}[\text{kW h}] + \$680 \quad (4)$$

$$\$C_{Batt,Li-ion} = \$651.2 * \text{energy}[\text{kW h}] + \$680 \quad (5)$$

$$\$C_{BattRep} = \frac{FV}{(1+i)^N} \quad (6)$$

where P_E is the peak power of the engine in kW, P_M is the peak power of the electric motor in kW, $\$C_{Batt,NiMH}$ is the cost of the Ni–MH batteries, and $\$C_{Batt,Li-ion}$ is the Li-ion batteries cost, energy represents the capacity of the battery pack in kW h, FV is the future value cost in dollars, i is the interest rate, assumed to be 7%, and N is the used time of battery in years, according to a 15 year, 150,000 mile vehicle life, Ni–MH and Li-ion will have a battery replacement at 100,000 miles (year 10) [6,17].

In addition, the vehicle performance requirements are defined as the constraints. The vehicle is required to meet four kinds of performance constraints for avoiding sacrificing the vehicle performance during optimization. Many of these constraints are taken from PNGV passenger car goals, while others are developed from

Table 1
Vehicle performance constraints.

Constraints	Description
Acceleration time	0–60 mph (0–97 km/h) ≤ 12 s 40–60 mph (64–97 km/h) ≤ 5.3 s 0–85 mph (0–137 km/h) ≤ 23.4 s with hybrid traction
Gradeability	0–30 mph (0–48.3 km/h) ≤ 5 s with motor-only traction 55 mph (88.5 km/h) at 6.5% grade for 1200 s with the SOC range of 0.2–0.7
Maximum speed	≥ 90 mph (145 km/h)
All electric range (AER)	10 miles (16 km), 20 miles (32 km), 40 miles (64 km) with ΔSOC ≤ 0.8 and Δtrace ≤ 2 mph (3.2 km/h) under UDDS

examining what consumers want when purchasing automobiles [18]. The performance constraints are shown in Table 1.

The optimal selection of component sizes can be defined as a constrained optimization problem as follows:

$$\text{Minimize } f(x) \text{ s.t. } g_i(x) \leq 0, i = 1, 2, \dots, n \quad (7)$$

where x is a solution to the problem, Ω is the solution space which defines the lower and upper bounds of variables, inequality $g_i(x) \leq 0$ is a group of non-linear constraints discussed above, $f(x)$ is the objective function and n is the number of constraints.

3.3. PCOA solution

The basic process of PCOA [11] generally includes two major steps. Firstly, define a chaotic sequence generator based on chaotic map, and then generate several sequences of chaotic points and map them to several sequences of design points in the original design space. Then, calculate the objective functions with respect to the generated design points and choose the point with the minimum objective function as the current optimum. Repeat this step until specified convergence criterion is satisfied. Secondly, the current optimum is assumed to be close to the global optimum after certain iterations, and it is viewed as the center with a little chaotic perturbation, and the global optimum is obtained through fine search. Repeat this step until the specified convergence criterion is satisfied, then the global optimum is obtained.

Four parameters are involved in solution vector $x = (S_{IC}, S_{EM}, N_{BM}, S_{BC})$. During optimization, the vehicle model is constructed by software ADVISOR and vector x . The vehicle performance tests, such as AER test, maximum speed test, gradeability test and acceleration test, are performed. If all the performance requirements are satisfied, then calculate the drivetrain cost, otherwise, reject the vector x . In addition, suppose the number of parallel chaos is p , each group of chaotic sequences includes four initial chaotic variables, $z_{i,1}^0, z_{i,2}^0, z_{i,3}^0, z_{i,4}^0, 0 \leq z_{ij}^0 \leq 1, (i = 1, 2, \dots, p, j = 1, 2, \dots, 4)$, which are selected randomly, and the fixed points 0.25, 0.5, 0.75 of the logistic map cannot be used as initial variables [19]. The lower bounds of the searched variables are denoted as a_j and $b_j, j = 1, 2, \dots, 4$. x^* is assumed to be the optimum solution and f^* is the corresponding value of objective function. The search procedure by PCOA can be described as follows:

Step 1: Initialize the number of the first chaos search, M_1 , the number of the second chaos search, M_2 , the number of parallel chaos, p , initial value of chaos variables, $0 < z_{ij}^0 < 1 (i = 1, 2, \dots, p, j = 1, 2, \dots, 4)$ and adjusting parameter, $\alpha_j (j = 1, 2, \dots, 4)$.

Step 2: Set $k = 0$ and $f^* = \infty$.

Step 3: Carry out parallel chaos search using the first carrier wave.

Do

$i = 1$

Do

$$x_{ij}^k = a_j + z_{ij}^k(b_j - a_j), j = 1, 2, \dots, 4.$$

Evaluate the constraints using ADVISOR.

If at least one constraint is not satisfied

$$f(x_i^k) = \infty$$

Else computing $f(x_i^k)$ using Eq. (1)

If $f(x_i^k) < f^*$, then $x^* = x_i^k, f^* = f(x_i^k)$

Else if $f(x_i^k) \geq f^*$, then give up x_i^k

$i = i + 1$

Loop until $i \geq p$

$$z_{ij}^{k+1} = 4z_{ij}^k(1 - z_{ij}^k)m \quad j = 1, 2, \dots, 4$$

$k = k + 1$

Loop until $k \geq M_1$

Step 4: Perform chaos search using the second carrier wave

Do

$$x_j^k = x_j^* + \alpha_j(z_j^k - 0.5), j = 1, 2, \dots, 4.$$

Evaluate the constraints using ADVISOR.

If at least one constraint is not satisfied

$$f(x_i^k) = \infty$$

Else computing $f(x_i^k)$ using Eq. (1)

If $f(x^k) < f^*$, then $x^* = x^k, f^* = f(x^k)$

Else if $f(x^k) \geq f^*$, then give up

$$x_j^k \cdot z_j^{k+1} = 4z_j^k(1 - z_j^k) \quad j = 1, 2, \dots, 4.$$

$k = k + 1$

Loop until $k \geq M_1 + M_2$

Step 5: Stop the search process and output x^* as the best solution.

4. Optimization results and discussion

4.1. Assumption and parameters setting

The base vehicle platform used for this study is a midsize sedan. The vehicle characteristics are given below in Table 2. The ADVISOR model of the optimized vehicle is built according to the base vehicle characteristics. In addition, the ADVISOR includes a routine program that allows the variation of component sizes through scaling of maps. Therefore, in order to implement component sizes continuously varying in search of an optimum combination, the selected baseline components will be linearly scaled as necessary by scaling factors to satisfy the design requirements.

Table 2
Base vehicle characteristics.

Parameter	Value
Glider mass	1150 kg
Cargo mass	136 kg
Gearbox	5-Speed manual gearbox Ratio: [2.84, 3.77, 5.01, 7.57, 13.45]
Frontal area (A_f)	2.17 m ²
Drag coefficient (C_D)	0.3
Wheel radius (r_r)	0.32 m
Rolling resistance coefficient (f_r)	0.01

For component sizing, the baseline IC engine of Geo Metro 1.0L SI engine with maximum power output of 41 kW and peak efficiency of 0.34 is used. The engine torque scaling factor, S_{IC} , is used to determine the engine size. In addition, for the baseline of electric motor, a 58 kW PM motor with 0.92 peak efficiency is employed. The motor torque scaling factor, S_{EM} , is used to determine the motor size. A 12 V 6 Ah Saft Lithium Ion battery and 6 V Ovonic 28 Ah Ni–MH battery are selected respectively as the baseline battery. The number of battery modules, N_{BM} , and the battery capacity scaling factor, S_{BC} , are used to determine the battery size. The range of the variations for each decision variable is determined based on the desired performance characteristics of components. In this pa-

Table 3
Upper and lower bounds of optimization variables for two types of battery.

Battery type	Optimization variable	Lower bound	Upper bound	
Ni–MH	S_{IC}	0.6	1.5	
	S_{EM}	0.6	1.5	
	N_{BM}	25	60	
	S_{BC}	PHEV10	0.6	1.2
	PHEV20	0.7	1.4	
	PHEV40	0.9	1.8	
Li-ion	S_{IC}	0.6	1.5	
	S_{EM}	0.6	1.5	
	N_{BM}	20	50	
	S_{BC}	PHEV10	2.1	3.1
		PHEV20	3	4.3
	PHEV40	5.3	6.3	

Table 4
Drive cycles specifications.

Drive cycle	UDDS	HWFET	LA92	US06
Maximum speed (km/h)	91	96	108	128
Average speed (km/h)	32	78	39	77
Distance (km)	12	17	16	13
Time (s/min)	1369/23	765/13	1435/24	600/10
Maximum acceleration (m/s^2)	1.48	1.43	3.08	3.76
Idle (s)	259	6	234	45

Table 5
Optimal parameters obtained based on the UDDS for two types of battery.

Battery type	AER (miles)	Optimization variables			
		S_{IC}	S_{EM}	N_{BM}	S_{BC}
Ni–MH	10	1.1473	0.8337	40.3988	0.7712
Li-ion	10	1.1045	0.8103	29.4113	2.4413
Ni–MH	20	1.1047	0.8626	38.3320	1.1022
Li-ion	20	1.0966	0.8441	27.6625	3.2781
Ni–MH	40	1.3665	0.8665	50.8268	1.6998
Li-ion	40	1.3012	0.8187	33.4731	5.7328

Table 6
Optimum PHEV specifications for two types of battery.

Battery type	AER (miles)	Curb mass (kg)	Motor power (kW)	Engine power (kW)	Battery energy (kW h)	P/E ratio (1/h)	Battery capacity (Ah)	Drivetrain cost (US\$)
Ni–MH	10	1593	48.4	47.0	5.23	12.36	21.6	\$5348
Li-ion	10	1556	47.0	45.3	5.17	14.67	14.6	\$8171
Ni–MH	20	1630	50.0	45.3	6.52	9.41	28.3	\$5904
Li-ion	20	1570	49.0	45.0	6.53	10.93	19.7	\$9543
Ni–MH	40	1821	50.3	56.0	14.5	5.61	47.6	\$9402
Li-ion	40	1716	47.5	53.3	13.82	6.25	34.4	\$16,766

per, the reference values of the optimized variables are firstly determined by the method proposed by the paper [6]. Then the range of the variations is determined by reducing or adding 40–50% of the reference values. The range is illustrated in Table 3. The adjusting parameter α is a very important parameter, and it adjusts small ergodic ranges around x^* . Here α is given (0.2,0.2,2.0,0.2) to make the algorithm have excellent performance in this study [20]. Considering comprehensively the computing time and optimization precision, the parameters M_1 , M_2 and p are set separately as $M_1 = 100$, $M_2 = 100$, $p = 5$.

Finally, AER is generally defined as the distance in miles that a fully charged PHEV can be driven by stored electricity before starting its engine [21]. Therefore, to simulating the constraint of AER, a pure electric control strategy is used. During the process, the vehicle is driven by electric motor without starting the engine. The initial SOC of battery is set to 1.0 and the minimum SOC is set to 0.2. For different AER, simulating corresponding driving cycle times is needed to judge if the constraint is satisfied by delta trace, which is the absolute difference in required speed of the cycle and the actual speed achieved by the vehicle. For example, simulating AER10 needs $1.342 \times$ UDDS driving cycle (the distance of $1 \times$ UDDS is 7.45 miles). During simulation, it is shown that the AER constraint is not satisfied if delta trace exceeds the specified value (2 mph). In addition, because hybrid drive is required for simulating other constraints, the control strategy of charge sustaining is used, which is a typical control strategy for hybrid drive in ADVISOR. The Urban Driving Dynamometer Driving Schedule (UDDS) is selected as test cycle and the Highway Fuel Economy Test (HWFET), LA92 and US06 are used to evaluate the sensitivity of optimum solutions to different cycles. Among them, the UDDS and HWFET represent urban and highway driving behaviors and the LA92 and US06 are more aggressive urban and highway driving cycles respectively. Table 4 shows the four drive cycle specifications.

5. Optimization results

The optimal parameters obtained based on the UDDS driving cycle and two types of battery are summarized in Table 5. Using these parameters and the selected baseline components, the final component sizes are determined. For example, the engine peak power is obtained via multiplying the engine torque scaling factor by the maximum power of baseline engine, that is $P_E = 41S_{IC}$.

Furthermore, the vehicle mass is the sum of the base vehicle mass and the optimized components mass including engine, electric motor and battery pack. The drivetrain cost is calculated by Eqs. (1)–(6). The corresponding PHEVs are summarized in Table 6. As it is shown by these results, the optimal design variables are changed for different AER and different battery type. As AER increases, more battery energy is needed and the vehicle mass is increased. Meanwhile, more power from the engine and electric motor is needed to drive the vehicle. Therefore, the drivetrain cost is enhanced with increased AER. In addition, for the same AER, the optimum PHEV using Li-ion battery is lighter than that using Ni–

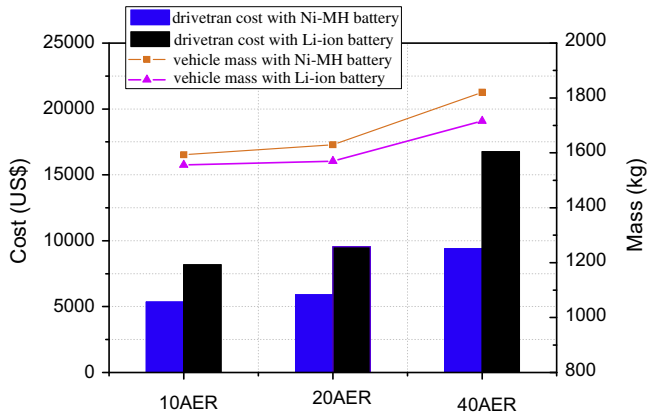


Fig. 2. Drivetrain cost and vehicle mass for different AER and battery.

Table 7 Performance characteristics of each design for two types of battery.

Battery type	Performance constraints	PHEV10	PHEV20	PHEV40
Ni-MH	Grade	6.8%	6.8%	10.5%
	0–97 time (s)	10.4	10.5	10.4
	64–97 time (s)	5.3	5.3	5.3
	0–137 time (s)	21.3	21.5	21
	Max. speed (km/h)	202.3	204.1	210.8
	AER (miles)	15.5	21.3	42
Li-ion	Grade	6.6%	6.8%	10.6%
	0–97 time (s)	10.5	10.4	10.5
	64–97 time (s)	5.3	5.3	5.3
	0–137 time (s)	21.4	21.3	21.2
	Max. speed (km/h)	202.3	203.9	207.7
	AER (miles)	15.8	20	41.2

MH battery. Moreover, less battery energy, and smaller engine size and motor size are required for smaller vehicle mass. However, the higher cost of Li-ion battery caused the corresponding drivetrain cost is higher than that using Ni-MH battery (shown in Fig. 2).

By using optimized components and ADVISOR, the corresponding vehicle model is constructed and the driving performance characteristics are obtained by simulation. The results are summarized in Table 7. It should be noted that the grade in this table is the vehicle gradeability under the conditions of 55 mph (88.5 km/h) for 1200 s with the SOC range of 0.2–0.7. These results confirm that the driving characteristics required previously are satisfied using the proposed approach.

In order to evaluate the effectiveness of the proposed approach for PHEV component sizing, the results using Ni-MH battery are compared with the results from the analysis-based optimization approach which has the following features [6]. Firstly, several combinations of the engine size and motor size are obtained by simulation software according to the acceleration performance constraint. And then, corresponding smooth function is obtained by data fitting, with which the relationship between motor and engine sizes is determined during the acceleration. Secondly, the

Table 8 Optimum designs for Ni-MH battery type in analytical-based optimization approach.

AER (miles)	Curb mass (kg)	Motor power (kW)	Engine power (kW)	Battery energy (kW h)	P/E ratio (1/h)	Battery capacity (Ah)	Drivetrain cost (US\$)
10	1743	45	50.5	5.61	10.84	24.6	5829
20	1787	46	52.5	7.50	7.89	33.8	6792
40	1958	50	56	14.60	5.59	47.7	10,352

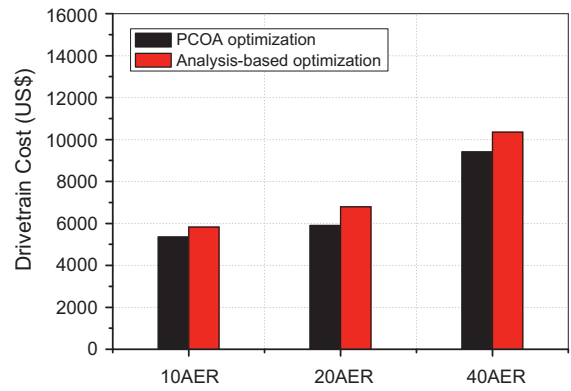


Fig. 3. Drivetrain cost for Ni-MH battery type with different approach.

minimum motor size and battery capacity are obtained using simulation software according to pure electric acceleration performance constraint. Finally, an optimization routine is used for optimizing the design parameters. The designed PHEV by analysis-based optimization approach for Ni-MH battery is shown in Table 8. The drivetrain cost obtained from the two approaches mentioned above is compared in Fig. 3. As it can be seen in this figure, the drivetrain cost optimized by the proposed approach is decreased.

5.1. Effect of performance constraints on component sizing

In order to study the sensitivity of the optimal component sizes to performance constraints, the acceleration and gradeability (0–60 mph (0–97 km/h) \leq 9 s, 65 mph (104 km/h) at 6% grade for 1200 s) [18], which is more attractive to customers, are used for component sizing. Other constraints are the same as given previously. Considering Ni-MH battery, the optimized component sizes are compared in Fig. 4. The obtained drivetrain costs and vehicle mass are compared in Fig. 5. In these two figures, P1 and P2 represent respectively different constraint requirements. P1 represents the common performance constraints (0–60 mph (0–97 km/h) \leq 12 s, 55 mph (88.5 km/h) at 6.5% grade for 1200 s) and P2 expresses the higher performance constraints (0–60 mph (0–97 km/h) \leq 9 s, 65 mph (104 km/h) at 6% grade for 1200 s). As it can be seen in the figures, for the same AER, the higher the performance is raised, the larger the component sizes should be and the corresponding higher cost and vehicle mass are obtained.

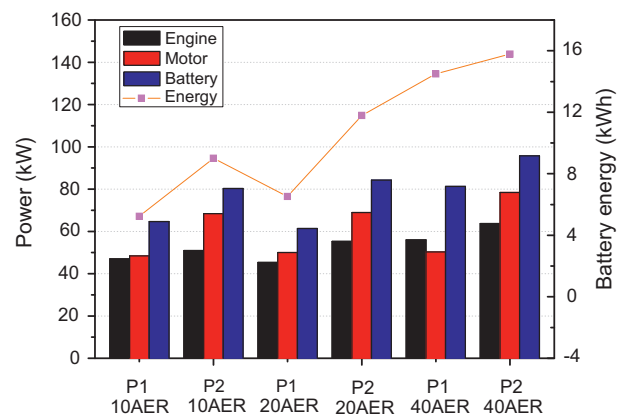


Fig. 4. Optimum component sizes for different performance constraints.

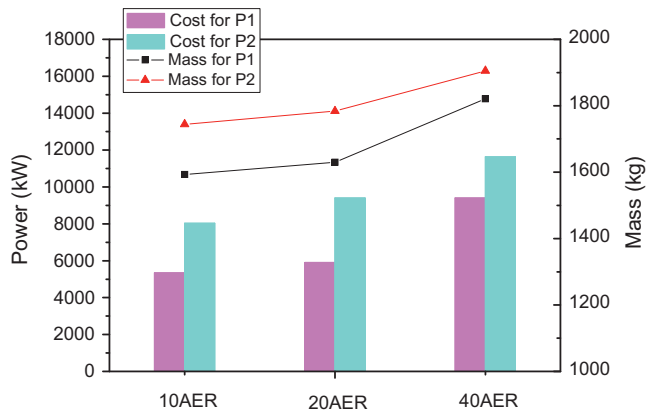


Fig. 5. Drivetrain cost and vehicle mass for different performance constraints.

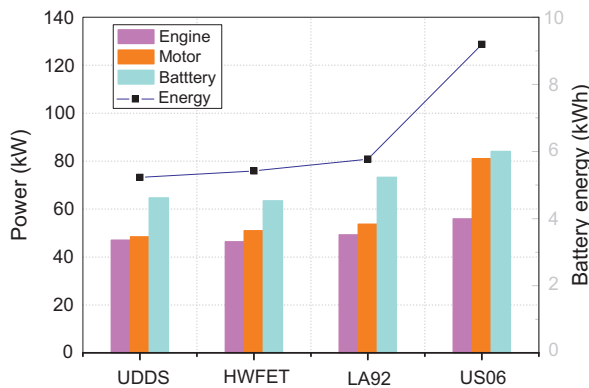


Fig. 6. Optimum component sizes for different driving cycles.

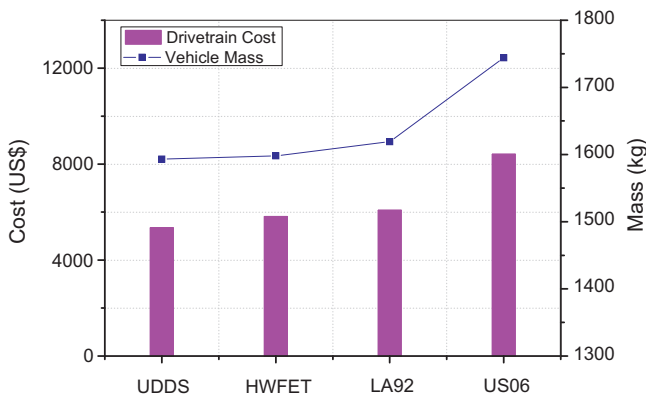


Fig. 7. Drivetrain cost and vehicle mass for different driving cycles.

5.2. Effect of driving cycle on component sizing

In order to study the effect of driving cycle on the component sizing, the optimization problem is also solved respectively for HWFET, LA92 and US06 driving cycles. For Ni–MH battery, 10AER and common performance constraints, the optimized component sizes are compared in Fig. 6. The obtained corresponding drivetrain costs and vehicle mass are compared in Fig. 7. As it can be seen in these figures, the power and energy of battery increases obviously with cycle aggressiveness, and accordingly, higher drivetrain cost and vehicle mass are obtained.

6. Conclusion

In this paper, a methodological approach for the optimization of PHEV component sizing is presented. This optimization problem is formulated based on PCOA method. The variables in PHEV component sizing include the IC engine, electric motor and energy storage system. The objective function is defined to minimize the drivetrain cost. The vehicle performance requirements are selected as the constraints. The optimization is performed for various AER and different battery types. The results show that Ni–MH battery-based vehicle produces less cost for AER of 10, 20, and 40 miles. Furthermore, the simulation results reveal that the proposed approach is effective in reducing drivetrain cost compared with previous approach. Finally, the effect of performance constraints and driving cycle on the optimization of PHEV component sizes is investigated. The simulation results show the sensitivity of component sizing optimization to the performance requirements and the driving cycle.

For a PHEV to be as efficient as it is possible, proper management on its different power elements is required. This task is performed by control strategy. Future research will be carried out with an emphasis on the simultaneous selection of component sizes and control parameters.

References

- [1] Huang KD, Quang KV, Tseng KT. Study of the effect of contraction of cross-sectional area on flow energy merger in hybrid pneumatic power system. *Appl Energy* 2009;86:2171–82.
- [2] Amjad S, Neelakrishnan S, Rudramoorthy R. Review of design considerations and technological challenges for successful development and deployment of plug-in hybrid electric vehicles. *Renew Sustain Energy Rev* 2010;14:1104–10.
- [3] Bradley TH, Frank AA. Design, demonstrations and sustainability impact assessments for plug-in hybrid electric vehicles. *Renew Sustain Energy Rev* 2009;13(1):115–28.
- [4] Simpson A. Cost-benefit analysis of plug-in hybrid electric vehicle technology. Paper presented at the 22nd international battery, hybrid and fuel cell electric vehicle symposium and exposition. Yokohama, Japan; 23–28 October 2006.
- [5] Sharer P, Rousseau A, Nelson P and Pagerit S. Vehicle simulation results for PHEV battery requirements. Obtained through the Internet: <http://www.afdc.energy.gov/afdc/progs/view_citation.php?10391/PHEV>.
- [6] Golbuff S. Optimization of a plug-in hybrid electric vehicle. M.S. Thesis. Georgia Institute of Technology.
- [7] Fellini R, Michelena N, Papalambros P, Sasena M. Optimal design of automotive hybrid powertrain systems. In: Proceedings of ECO Design 99 – first int. symposium on environmentally conscious design and inverse manufacturing, Tokyo, Japan; February 1999.
- [8] Fefferies DJ, Deane JHB, Johnstone GG. An introduction to chaos. *Electron Commun Eng J* 1989;1(3):115–23.
- [9] Li B, Jiang WS. Optimizing complex functions by chaos search. *Cybern Syst* 1999;29(4):409–19.
- [10] Luo YZ, Tang GJ, Zhou LN. Hybrid approach for solving systems of nonlinear equations using chaos optimization and quasi-Newton method. *Appl Soft Comput* 2008;8:1068–73.
- [11] Liang H, Gu X. A Novel chaos optimization algorithm based on parallel computing. *J East China Univ Sci Technol* 2004;30(4):450–3.
- [12] Markel T, Brooker A, Hendricks T, Johnson V, Kelly K, Kramer B, et al. ADVISOR: a systems analysis tool for advanced vehicle modeling. *J Power Sources* 2002;110(222):255–66.
- [13] Wipke KB, Cuddy MR, Burch SD. ADVISOR 2.1: a user-friendly advanced powertrain simulation using a combined backward/forward approach. *IEEE transactions on vehicular technology: special issue on hybrid and electric vehicles*; 1999.
- [14] Bradley TH, Frank AA. Design, demonstrations and sustainability impact assessments for plug-in hybrid electric vehicles. *Renew Sustain Energy Rev* 2009;13:115–28.
- [15] Graham R, et al. Comparing the benefits and impacts of hybrid electric vehicle options. *Electron Power Res Inst (EPRI)*; 2001.
- [16] Duval M, et al. Advanced batteries for electric-drive vehicles: a technology and cost-effectiveness assessment for battery electric vehicles, power assist hybrid electric vehicles and plug-in hybrid electric vehicles. *Electron Power Res Inst (EPRI)*; 2004.
- [17] ThermoAnalytics, Inc. Battery types and characteristics; April 2006 <<http://www.thermoanalytics.com/support/publications/batterytypespec.doc.html>>.
- [18] Moore TC, Lovins AB. Vehicle design strategies to meet and exceed PNGV goals. Future transportation technology conference. SAE paper no. 951906.